Atmospheric Particles in Kermanshah, Iran

Häggström, Rebecka
tfy12rha@student.lu.se

July 3, 2017

Abstract

No measurements of airborne particles have been done in Iran previously. Starting characterization of aerosol particles in a completely new geographical area, a suitable and important measurement parameter is the aerosol particle number size distribution. This can be used to indirectly infer climate- and health effects of the particles. These measurements are often accomplished with the help of an SMPS (Scanning Mobility Particle Sizer) instrument. A collaboration between Lund University and Razi University located in the large town Kermanshah in Iran was initiated. A previously used SMPS system in the Lund University laboratory was set up. Students at Razi University were trained to construct an SMPS system of their own to be used in Kermanshan by mimicking the Lund SMPS instrument.

Measurements in Kermanshah were performed with a PSAP (Particle soot absorption photometer) at an urban background environment and at street level. This instrument determines the black carbon particle concentration through the light absorbing properties. In this way it can help determine part of the chemical constituent in particles, which are detrimental for human health through inhalation in the respiratory tract.

The black carbon mass concentrations at street level were 0.1 and 0.6 ug/m^3 during a three hour measurement period during two different days in February 2017. In the urban background environment the concentrations were close to zero during three different days in November 2016. The reason for the distinctly different measurement values in February at street level could not be concluded based on the short time period of measurement.

Acknowledgement

Firstly, I would like to thank my supervisors Adam Kristensson and Arash Gharibi for all the effort they have put in to help me with the project and this report. I would not have been able to do this without their never ending support and knowledge.

I would also like to thank Patrik Nilsson for all the help he has given me with the laboratory work.

A big thanks also to the research group at Razi University, and especially to Parisa Kahari, for the PSAP data and help with understanding the measurement process used.

Lastly, I would like to thank my boyfriend Markus Maga for the support and encouragement he has given me over the course of this process.

Contents

1 Introduction

1.1 Background

Airborne particles affect both the climate and human health. They are hazardous to inhale and have a cooling effect on the climate, hence counteracting global warming (SMHI 2011). To map the particle concentrations globally is therefore important.

In the Middle East, only a few measurements on air pollution have been done, and even fewer on airborne particles. Measurements have been done in the capital of Jordan, Amman, (Hussein et al. 2011) and in rural areas in the western parts of the Middle East (Lihavainen et al. 2016), and several Arab countries in west Asia (Roumie et al. 2016). These have all shown high levels of pollution, $75 \cdot 10^3$ to $120 \cdot 10^3$ particles/cm^3 during traffic rush hours (Hussein et al. 2011), and PM10 of 95 µg/m^3 and PM2.5 of 33 µg/m^3 at ambient conditions (Lihavainen et al. 2016). No measurements of airborne particles have been done in Iran, but nothing suggests that the levels would be lower there.

1.2 Purpose

The Division of Ergonomics and Aerosol Technology and the Division of Nuclear Physics at Lund University wanted to start long term measurements of aerosols in Iran. To do this Lund University wanted to start a collaboration with an Iranian university, so Razi University was reached out to. Razi were interested, so it was decided that the measurements should take place there. The contact between the universities was set up and maintained by Arash Gharibi, who is affiliated with Lund university. The budget for this project was low, so it was agreed to initiate the measurements in Iran with the help of a diploma work in Lund, which resulted in this project report. Also old and broken instruments were loaned to Razi where they were repaired and serviced to working condition. Razi university eventually had all the components needed to set up a scanning mobility particle sizer (SMPS), which is a high precision instrument that is used to measure the particle number size distribution. A particle soot absorption photometer (PSAP) was also borrowed to measure the soot particle mass concentration.

The main purpose is to start long-term measurements of the number and mass size distribution and soot particle mass concentration of airborne particles outside Razi University in Kermanshah, Iran. The results from the measurements will show the particle concentrations, which in turn will indicate how much the particles affect the health of the population, how they affect the climate, and what the sources of the particles are. It is believed that the main sources are industries, traffic, and dust from the desert (Hussein et al. 2011; Roumie et al. 2016; Lihavainen et al. 2016; NASA 2017)

Before the SMPS in Iran could be put together, an old SMPS system, similar to the one in Iran, in Lund was repaired and serviced to working condition. With this experience Razi could be instructed on how to set up the SMPS

system in Iran. Routines for how to calibrate the instruments in Iran will also be established. Some initial measurements with the PSAP are to be taken in Kermanshah to give a first insight to the particle concentrations there. The goal is to have the measurements in Kermanshah running for decades to come.

2 Theory

2.1 Aerosols

An aerosol is a collection of liquid or solid particles suspended in air. To be regarded as aerosols the particles need to be airborne long enough to be observed or measured. The size range of aerosols is approximately 0.001 to 100 µm. Examples of aerosols are airborne dust particles, soot from combustion processes, pollen, salt particles formed from ocean spray, and clouds. How they affect the climate and human health vary greatly depending on their physical and chemical properties (Hinds 1999a).

The size of the aerosol is important as all aerosol properties depend on it. Even the equations describing various aerosol properties may change with the particle size, since the aerosol size ranges over five orders of magnitude. Often equivalent diameters and correction factors are used to apply different aerosol theories to non-spherical particles. An equivalent diameter is the diameter of a sphere with the same value of a specific physical property as the non-spherical particle. (Hinds 1999a)

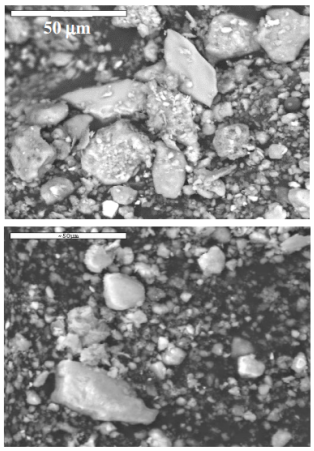

Figure 1: BSE image of particles collected during two different dust storms (Blanco et al. 2003).

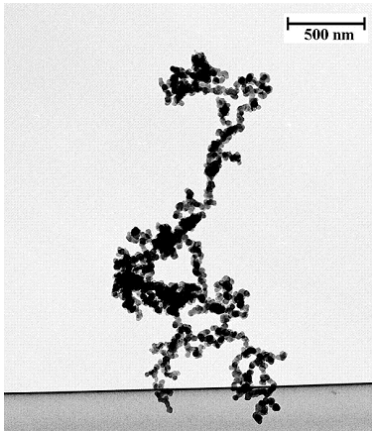

Figure 2: TEM image of a soot particle (Gharibi 2006).

About 40 % of the mass of aerosols in the troposphere, the atmospheric layer closest to the earths surface, are coarse dust particles generated by wind erosion. This mainly occurs in dry and barren regions where little to no vegetation exists that protects the ground from the erosion. The erosion happens when strong winds lift loose sand and dust particles up from the ground into the atmosphere. The lifetime for dust in the atmosphere ranges from a few hours to several days depending on the particle size. (Terradellas, Nickovic, and Zhang 2015)

Particles from traffic are either exhaust particles or non-exhaust particles. Exhaust particles are generated from the combustion of the fuel, either directly in the combustion process like soot particles or like secondary particles from volatile organic compounds (VOC). Non-exhaust particles are generated from the brakes, tires, en-

gine wear, and resuspension from the road. The mass of particulate matter from exhaust and non-exhaust sources are about the same. Particle emissions from vehicles make up a large part of the number concentration of the ultrafine particles in an urban environment. The primary particles from the vehicles are mainly soot agglomerates in the range of 40 to 100 nm, while the secondary particles range between 3 and 30 nm. The emissions take place at ground level and are therefore frequently inhaled by humans. (Tiitta 2009)

The particles emitted from industries vary greatly depending on which industry it is. An industry that produces power from combustion of, by example, coal or oil will produce particles very similar to traffic. A paper mill on the other hand will emit a different composition of particles, and an iron mill will also have a different emission profile. A combined Iron and steel mill, which is an industry present in Iran, emits particles mainly consisting of different metal elements, like Fe, Pb, Zn, and Ni. The emission profile has modes at 0.45 µm, 4 µm, 6 µm, and 1.2 µm (Dall'Osto et al. 2008).

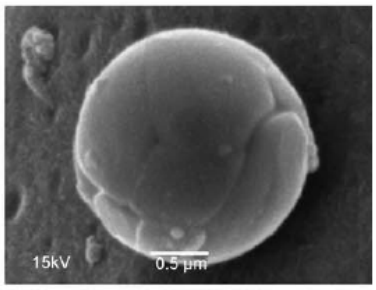

Figure 3: SEM photomicrograph of an airborne iron particle (Xie et al. 2005).

The atmospheric organic particles emitted from fossil fuel combustion and dust particles can work as nuclei for cloud formation, depending on their size, shape and composition. Alteration of the droplets of the clouds affects their capacity to absorb solar radiation, hence changing how much of the radiation that reaches earths surface. The particles also affect the growth of cloud droplets, thus influencing the amount and position of rainfall (Terradellas, Nickovic, and Zhang 2015). Apart from the droplet formation, soot particles emitted from fossil fuel combustion and dust particles are regarded as relatively good ice nucleation for ice cloud formation (Huang et al. 2014). Dust and soot particles are also warming the climate through absorption of solar radiation. The dust particles are also able to reflect incoming solar radiation, thus contributing to a cooling effect (Huang et al. 2014).

Airborne particles are a big health risk for humans. Particles can enter the lungs through inhalation and deposit there. Particles of certain sizes deposits deeper in the lung where they do more harm. Most of the coarse particles (larger than 2.5 µm) and ultra fine particles (smaller than 0.01 µm) deposit higher up in the respiratory system, in the head airways and tracheobronchial regions, due to impaction and diffusion respectively. Particles between 0.1 and 1 µm does not deposit to a large extent, but are mainly exhaled again. The alveolar region is where the exchange to the blood stream takes place, particles between 0.01 and 0.1 µm mainly deposit (Hinds 1999b). Mortality, hospitalization and disease are interdependent with levels of particulate matter (PM) in the air. An increase of PM10 (PM for particles with diameter less than 10 µm) by 10 % raises the mortality by around 1 % (Kristensson 2003). Globally, 3 million

premature deaths are caused by outdoor airborne particles with a diameter of 10 µm or smaller, with the majority of those deaths occurring in middle- and low-income countries (WHO 2017). The primary health effects on humans are cancer, cardiovascular and pulmonary diseases, asthma, and reduced lung function (Kristensson 2003).

2.2 SMPS

The scanning mobility particle sizer (SMPS) measures the particle number size distribution in a sample. The most simple set up for an SMPS system is depicted in figure 4.

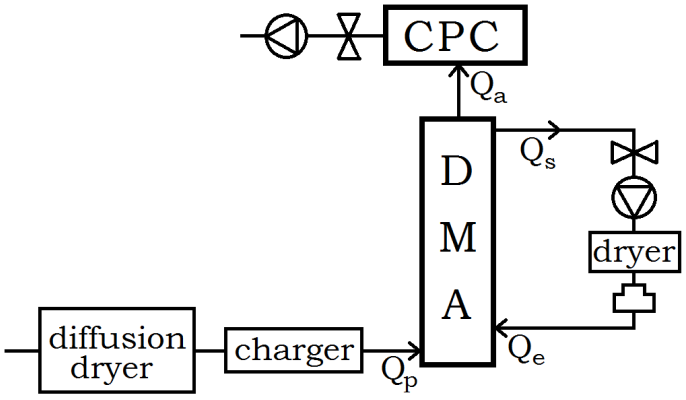

Figure 4: Schematic of the most simple SMPS set up. Here Q_p is the sample flow, Q_a is the flow with the chosen particles, Q_a is the excess flow and Q_e is the sheath flow

The three main parts of the SMPS are the charger, the differential mobility analyzer (DMA), and the condensation particle counter (CPC). A polydisperse aerosol (an aerosol consisting of particles of several sizes) enters the SMPS. It passes through the diffusion dryer to remove all excess water from the flow. Thereafter, it passes through the charger which charges the particles to a known charge distribution. Then the aerosol enters the DMA, which selects particles of one electrical mobility, i.e. the speed with which the charged particles travel through an electrical field. Thereafter the aerosol enters the CPC which counts the particles, giving a number concentration for the incident aerosol flow.

If the charge of a particle is known, it is possible to determine the particles' size from measurement of its electrical mobility. Hence it is vital to be able to produce a known charge distribution to conduct characterization of the electrical mobility. There are two main types of chargers: the unipolar charger and the bipolar diffusion charger. The unipolar charger gives all the charged particles the same polarity while the bipolar diffusion charger, sometimes called an aerosol

neutralizer, produces charged particles of both polarities. The fraction, P, of particles of size d_p in nanometers that carries i charges is given by: (Flagan 2011)

$$P(d_p, i) = 10^{\sum_{j=0}^{5} a_{j,i}(log_{10} d_p)} \tag{1}$$

where the the parameter $a_{j,i}$ is given in table 1.

k	-2	-1	0	1	2
$a_{0,k}$	-26.3328	-2.3197	-0.0003	2.3484	-44.4756
$a_{1,k}$	35.9044	0.6175	-0.1014	0.6044	79.3772
$a_{2,k}$	-21.4608	0.6201	0.3073	0.4800	-62.8900
$a_{3,k}$	7.0867	-0.1105	-0.3372	0.0013	26.4492
$a_{4,k}$	-1.3088	-0.1260	0.1023	-0.1553	-5.7480
$a_{5,k}$	0.1051	0.0297	-0.0105	0.0320	0.5049

Table 1: The coefficients $a_{j,i}$ (Flagan 2011).

In the DMA the particles are separated depending on their electrical mobility. In figure 5, an illustration of a DMA cross section can be seen.

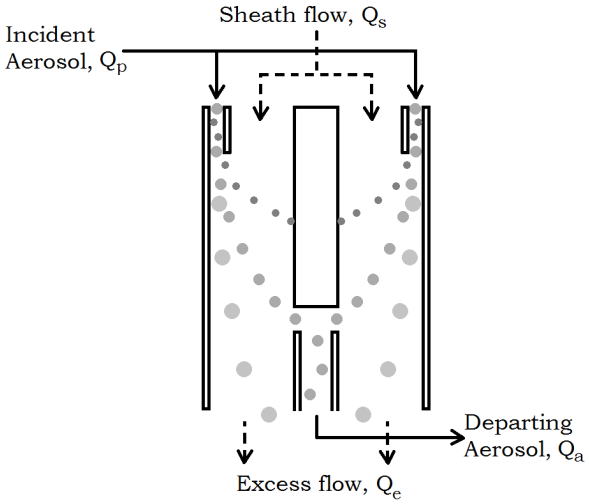

Figure 5: Illustration of the principles of a DMA.

A voltage is applied on the rod in the middle of the DMA. This produces a symmetric electric field which causes the charged particles to move towards the rod. If they move at the right speed, they will leave the DMA through a slit. How fast the particles move towards the middle of the DMA depends on the field strength and the electrical mobility of the particle. The electrical mobility, denoted Z, is given by: (Flagan 2011)

$$Z = \frac{ieC_c(Kn)}{3\pi\eta d_p} \tag{2}$$

where i is the number of charges, $e = 1.609 \cdot 10^{19}C$ is the elementary charge, η is the gas viscosity, d_p is the equivalent particle diameter, and $C_c(Kn)$ is the Cunningham slip correction factor, depending on the Knudsen number, which in turn is given by: (Flagan 2011)

$$C_c = 1 + Kn \cdot (\alpha + \beta \cdot e^{-\frac{\gamma}{Kn}}) \tag{3}$$

where the coefficients $\alpha = 1.142$, $\beta = 0.558$, and $\gamma = 0.999$ are experimentally determined. The Knudsen number is given by: (Flagan 2011)

$$Kn = \frac{2\lambda}{d_p} \tag{4}$$

where λ is the mean free path in the medium. For a set up where the sheath flow, Q_s, is equal to the excess flow, Q_e, and hence the two aerosol flows are the same, the mobility can also be expressed as (Flagan 2011):

$$Z = \frac{Q_s ln(r_1/r_2)}{2\pi VL} \tag{5}$$

where r_1 is the inner diameter of the DMA, r_2 is the outer diameter, V is the voltage on the inner rod, and L is the length of the DMA. (Flagan 2011). Combining equation 2 and 5, an expression for how the applied voltage corresponds to the particle diameter is produced:

$$V = \frac{3\pi\eta d_p}{ieC_c(Kn)} \cdot \frac{Q_s ln(r_1/r_2)}{2\pi L} \tag{6}$$

This way, a specific particle size can be selected by changing the voltage on the DMA through the voltage supplier.

The CPC counts the particles of one electrical mobility departing from the DMA. The incoming aerosol passes through a saturator block where alcohol evaporates into the aerosol flow, saturating it with vapor. The flow then moves into a condenser tube where the alcohol condenses onto the particles. This makes all the particles large enough to be detected by light-scattering. The enlarged particles pass through laser light, and light scatters off them. The scattered light is redirected to a photo detector, which converts the light to electric pulses that serves as counts of the particles (TSI 1999).

A computer with a LabVIEW program is used to control the set up. The computer is connected to the voltage supplier and the CPC through a DAQ-card. Through the data acquisition card (DAQ-card), the computer reads the counts from the CPC and controls the voltage scanning of the voltage supplier.

The data inversion for the SMPS is very complex. This is due to the continuous scanning of the voltage in the SMPS. The process for this is in depth described by Wang and Flagan (Wang and Flagan 1990) and is implemented in the LabVIEW program to give the correct particle diameter for each applied

voltage. The inversion takes into account the transport time inside the DMA and the applied voltage change during this transport, the smearing time (the delay time inside the CPC due to the flow mixing inside it), counting time (the time slot when the CPC accumulates counts) and counting efficiency (the efficiency for the CPC counting of particles depending on their size) of the CPC, the sampling line losses, the tube plumbing delays, and the DMA transfer function regarding DMA diffusion broadening and losses.

2.3 PSAP

Black carbon is emitted in incomplete combustion processes. Black carbon is only 10 % of the mass concentration of aerosols in the atmosphere in Europe, yet it has a large positive radiative forcing. (Zanatta et al. 2016)

Black carbon absorbs light over the whole solar spectrum. A filter based method is most often used to measure aerosol light absorption. The filter is used to sample ambient air. A light source and photo detector is used to measure the change in filter transmittance, or reflection, due to deposited particles on the filter. The Particle Soot Absorption Photometer (PSAP) is such a filter based instrument, which is commonly used. (Arnott et al. 2006)

To calculate the mass concentration of black carbon in the air, the absorption coefficient, σ_{ap}, for a specific wavelength, λ, is divided with the mass absorption cross-section, MAC, for λ: (Zanatta et al. 2016)

$$m_{EC} = \frac{\sigma_{ap}^{\lambda}}{MAC^{\lambda}} \tag{7}$$

This is only valid for wavelengths where the absorption is dominated by black carbon. The MAC-value is usually given for the wavelength 637 nm. (Zanatta et al. 2016)

The PSAP, though, measures the attenuation coefficient, σ_{atn}^{λ}, and not the absorption coefficient. This can be converted to the needed value using the Bond correction. The raw absorption coefficient $\sigma_{ap,raw}^{\lambda}$ can be derived from σ_{atn}^{λ} by: (Zanatta et al. 2016)

$$\sigma_{ap,raw}^{\lambda} = \frac{\sigma_{atn}^{\lambda} - K_1 \sigma_{sp}}{K_2} \tag{8}$$

where K_1 and K_2 are constants, and σ_{sp} is the scattering coefficient for the aerosol. The product $K_1\sigma_{sp}$ corrects for light scattering from the aerosol being read as absorption, and K_2 corrects for multiple scattering. The PSAP can operate on many different wavelengths, though 525 nm is a usual one. For this wavelength $K_1 = 0.02$ and $K_2 = 1.22$. (Zanatta et al. 2016)

The raw absorption factor need to be converted from the wavelength of the PSAP to 637 nm. This is done with: (Zanatta et al. 2016)

$$\sigma_{ap,raw}^{\lambda_2} = \sigma_{ap,raw}^{\lambda_1} \left(\frac{\lambda_1}{\lambda_2} \right)^{AAE} \tag{9}$$

where λ_1 is the wavelength of the PSAP, $\lambda_2 = 637$ nm, and $AAE = 1$ is the absorption Ångstrom exponent of unity. Lastly, to get the accurate absorption coefficient, σ_{ap}^{λ} a correction factor for the PSAP, CF_{PSAP}, needs to be applied: (Zanatta et al. 2016)

$$\sigma_{ap}^{\lambda} = \frac{\sigma_{ap,raw}^{\lambda}}{CF_{PSP}} \tag{10}$$

3 Method

3.1 The Lund SMPS System

The SMPS is set up to perform first an up scan, and then a down scan of the voltage in the DMA. The DMA is a single Vienna type DMA with inner radius 2.5 cm, outer radius 3.3 cm and length 28 cm. The CPC used is a TSI 3025A Ultrafine condensation particle counter. It has a built in pump, and regulates its own flow. The aerosol flow is set to 1.5 l/min, this flow then splits in three in the CPC: a bypass flow of 1.2 l/min, a sheath flow of 0.27 l/min and one flow of 0.03 l/min that enters the optics where the particles are detected.

The DMA is set up with a closed loop system for the sheath and excess flows, described by Jokinen and Mäkelä (Jokinen and Mäkelä 1996). This loop contains a filter, so no particles enter the DMA through the sheath flow, a pump, a dryer, and a needle valve. The needle valve will act as a critical orifice, keeping the flow through the loop nearly constant (Hinds 1999c). The pump is tested according to appendix A and the sheath flow is set to 8 l/min.

A DAQ-card 3036A is used to connect the instruments to the computer where LabVIEW 8.6.1 is run. The calibration curve for the CPC that is used needs to be entered into the program, to give true particle concentrations. This particular model of CPC does not need to have the internal temperatures controlled, but manages that itself. But if the temperatures need to be controlled, a direct connection between the computer and CPC can be set up.

The SMPS was tested and calibrated to make sure that it performed to the desired level. The procedures for this are described in detail in appendices B, C, and D.

3.2 The measurement site in Iran

Due to technical problems and delays, measurements in Iran could only be performed with the local PSAP. The PSAP has not yet been calibrated locally and operates at the wavelength 525 nm.

The measurement site in Kermanshah represents the exposure to particles in a typical Iranian urban area. Kermanshah, the capital of Kermanshah Province, is located in the west of Iran and is marked on the map in figure 7. Kermanshah has about 850,000 inhabitants, making it a fairly large city. Kermanshah has a moderate and mountainous climate and its climate is classified as a hot summer Mediterranean climate. Due to its altitude and exposed location to western winds, Kermanshah has high levels of precipitation.

The PSAP was placed both at street level and at an urban back ground site to take measurements over 3 hour periods. The street level measurements were performed in Golrizan boulevard, in the center of Kermanshah, and the urban background site is at Taghebostan which is located just north of the city. Both these locations are marked in figure 6.

Due to there only being one PSAP, the measurements were taken at different dates for the two sites. The urban background was measured 2016/11/27 be-

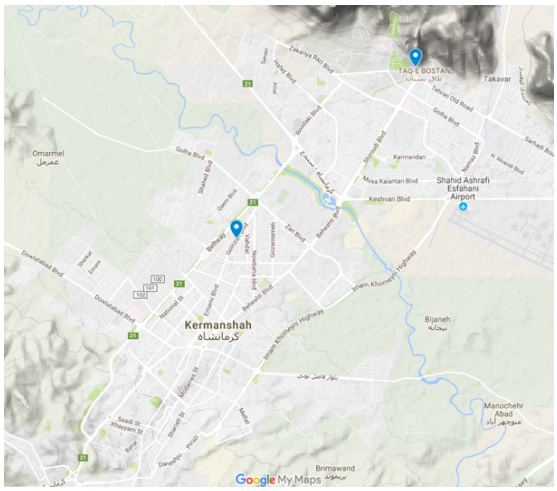

Figure 6: Map over Kermanshah with the two measurement sites market out with Golrizan boulevard in the middle and Taghebostan in the north.(Map data: Google)

Figure 7: Map over Iran with Kermanshah marked with a red dot (Dedering 2008).

tween 09:50 and 12:50 and 2016/11/29 between 09:00 and 12:00, and 2016/12/07 between 10:45 and 13:45 local time. The street level measurement was taken 2017/02/16 between 10:15 and 13:15, and 2017/02/28 between 10:15 and 13:15 local time.

4 Result and discussion

4.1 The Lund SMPS System

Since the TSI UCPC 3025A has a low flow through the optics where the particles are detected, the measured size distributions become very noisy. This can be reduced by averaging several consecutive measurements. On the other hand this leads to a lower time resolution.

The size calibrations for the SMPS were performed with Polystyrene Latex (PSL) spheres of 100 nm, 200 nm, and 500 nm. The SMPS shows a 10-15 % larger particle size than the one actually generated. This is not ideal, but within acceptable perimeters, though it is important to note this when using the instrument for future measurements.

In figure 8, the curves for the PSL 100 nm spheres are plotted. The scan time is set to 3 minutes for one up or down scan. In figure 8a the raw concentration can be seen. The peaks for the up scan and down scan coincide, which is important. If they do not, there is something major at fault with the SMPS, either with the instruments or the settings. The peak for this scan is at 113 nm. The lower peak at about 80 nm is due to the doubly charged incident particles. The plot for the inverted concentration is shown in figure 8b.

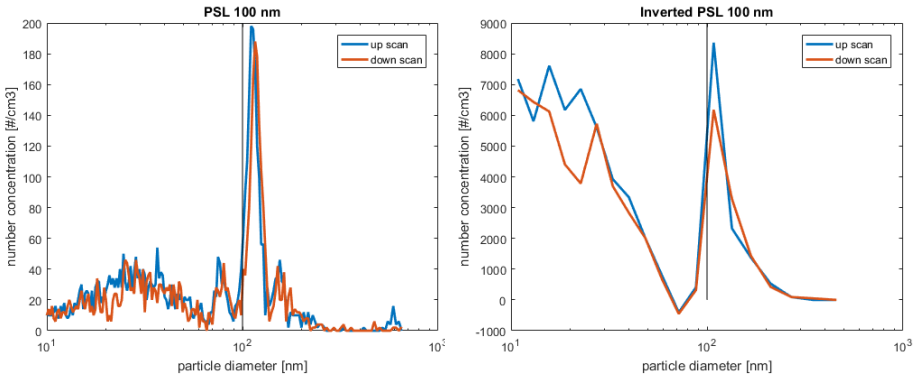

(a) Plot of the raw concentration.

(b) Plot of the inverted concentration.

Figure 8: Plots of the measured concentration of generated aerosol with 100 nm PSL particles. The vertical line in the figures indicates the actual size of the particles, 100 nm.

The graphs for the measurement of 200 nm PSL particles are displayed in figure 9. Figure 9a shows the raw concentration, with the main peaks at 222 nm for the up and 228 nm for the down scan. This is not a perfect overlap, but it is close enough to be acceptable. The peak at approximately 150 nm is due to doubly charged particles. I have not been able to figure out the reason for the peak at 500 nm diameter during up scans. It did show up during all the, about 10, performed up scans for the generated 200 nm aerosol. The inversion

of the concentration is shown in figure 9b.

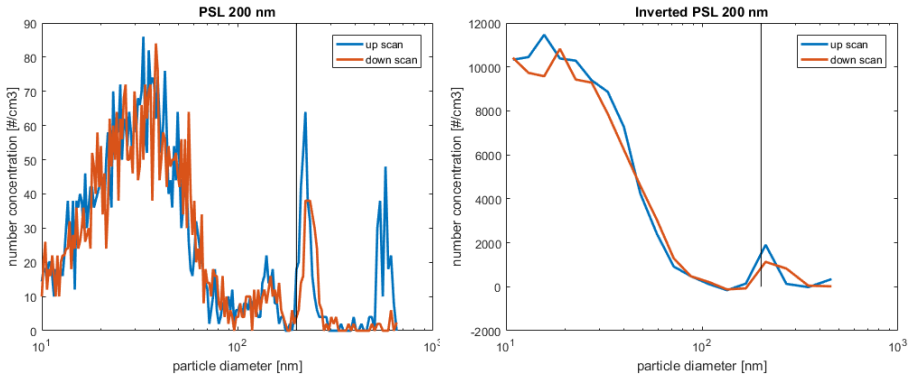

(a) Plot of the raw concentration. (b) Plot of the inverted concentration.

Figure 9: Plots of the measured concentration of generated aerosol with 200 nm PSL particles. The vertical line in the figures indicates the actual size of the particles, 200 nm.

Figure 10 displays the graphs for the measurements of 500 nm PSL particles. The peak from the particles in figure 10a is at 570 nm for both the up and down scan. In the plot for the inverted concentration in figure 10b, the curve ends before it even reaches 500 nm, which means that it is not possible to see the peak for these PSL particles in this graph. The reason for this is that the inversion decreases the interval.

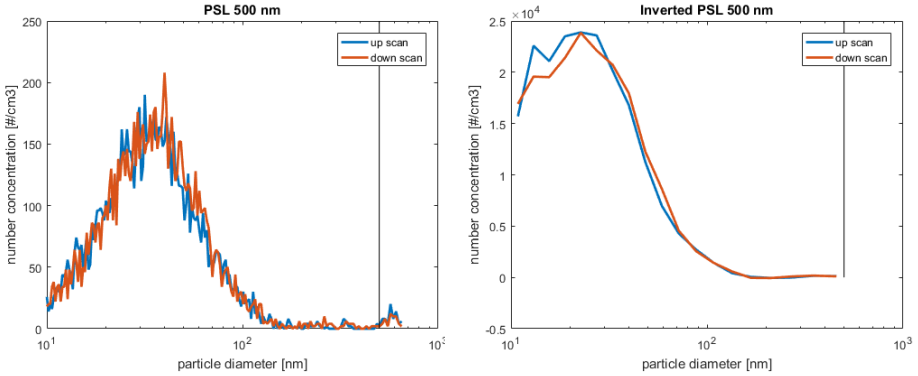

(a) Plot of the raw concentration. (b) Plot of the inverted concentration.

Figure 10: Plots of the measured concentration of generated aerosol with 500 nm PSL particles. The vertical line in the figures indicates the actual size of the particles, 500 nm.

Figure 11 shows four graphs from measurements of the indoor air in the

aerosol lab in Lund. The raw concentration can be seen in figure 11a, which displays one up and one down scan in different colors, and figure 11b, which displays the averaged concentration over two scan cycles (up-down up-down). There is considerably less noise in the averaged graph, as expected, though the time resolution is decreased from 3 minutes down to 12. Figures 11c and 11d show the inverted concentrations for the non-averaged and averaged raw concentrations respectively.

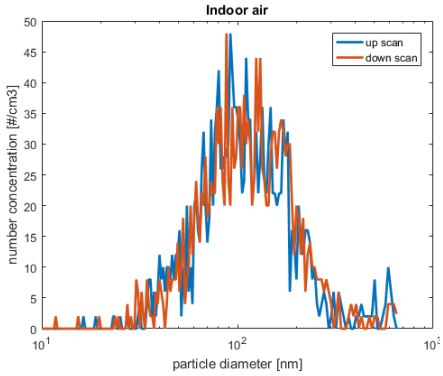

(a) Plot of the raw concentration.

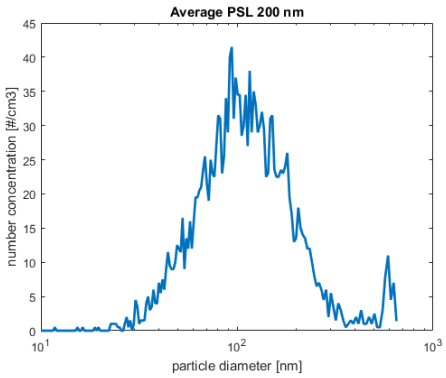

(b) Plot of the averaged raw concentration over two measurement cycles.

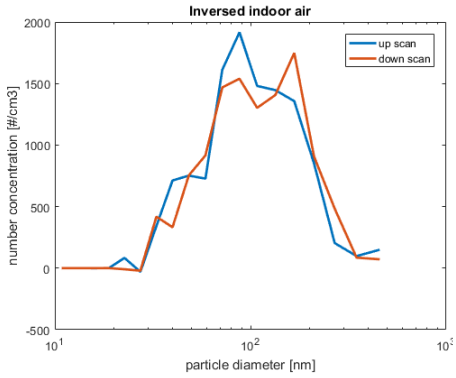

(c) Plot of the inverted raw concentration.

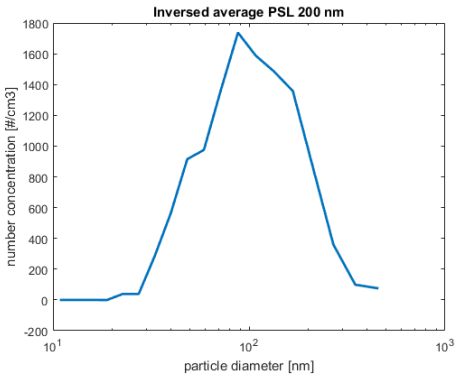

(d) Plot of the inverted averaged concentration.

Figure 11: Plots of the measured concentration of the ambient indoor air in the aerosol lab in Lund.

The aerosol number concentration measured with the SMPS in the aerosol lab was 1070 particles/cm^3 while the concentration measured with only the UCPC was 1450 particles/cm^3. The measurements were done several more times, and the SMPS constantly measures about 30 % lower concentrations than the UCPC irrespective of time and concentration. I have not been able to find out what this big particle loss is due to.

4.1.1 Further improvements of the Lund SMPS

The SMPS set up in Lund is in working order now, though it has some major weaknesses.

The first weakness is the low level of counted particles through the SMPS compared to what the CPC detects on its own. The cause of the low levels should be investigated as well as how it can be fixed. I can think of three different reasons for the low concentrations: 1 a particle loss in the DMA or the tubing, 2 the inversion not compensating enough for particle losses or, 3 the charger not charging the particles to the predetermined charge distribution.

The next weakness is that you have to choose between high noise levels or a low time resolution. This could be solved by changing the CPC to one that has a higher internal aerosol flow. There is also a function in the LabVIEW program to increase the measurement time for each particle size. This would also decrease the noise, but also still result in a low time resolution. This function does not work properly, though, so it could be valuable to try to repair.

Lastly, the weakness of characterizing the particles diameter as 10-15 % larger than it actually is. There is value in investigating why this is and trying to fix it. Possible causes are that the dimensions for the DMA differ between the actual DMA and the input in the program, or the DMA not managing to apply the correct voltage quick enough.

4.2 Measured levels of soot i Kermanshah

Figure 12 shows the attenuation coefficient measured with the PSAP for the two different sites, the street level site and the urban background site, at two of the dates over the times the measurements took place.

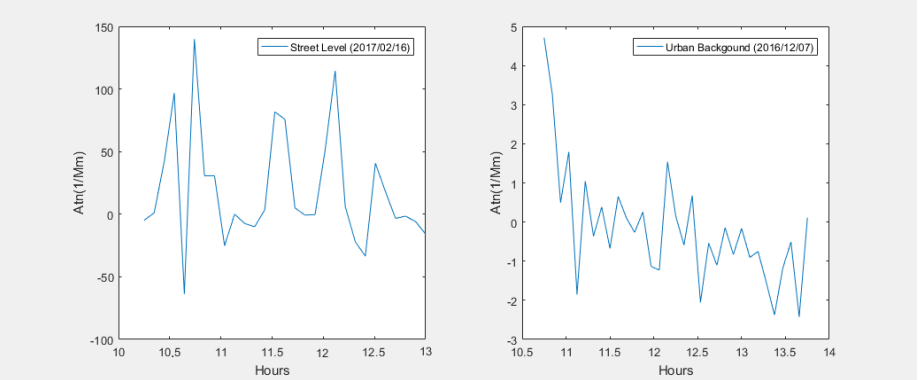

Figure 12: Graphs over the attenuation coefficient over the time it was measured with the PSAP.

The measured attenuation coefficient is fluctuating a lot for both the sites, and is negative for a lot of the measurement on the background site and some on

the street level site. This is probably due to it not being calibrated. One possible reason for this is the filter getting a high pressure and curve when mounted, and becoming more flat during the measurement. This can be examined by trying to insert the filter several times and noting if it makes a difference, as well as letting the measurement take place over several hours and seeing if it evens out later on. An other possible reason is that the light sources are not positioned correctly, and this is easily checked by just looking at them. But most important is to take a closer look at the instrument to determine what is the problem with it, and performing tests with generated soot particles, zero-particle filters and so on.

The urban background has a slight downwards trend, which can be a sign of higher concentrations even there during the rush hours earlier in the day. The street level measurements do not have a trend, and the urban background is also relatively constant in the later part of the measurement, which is expected since they are taken over the middle of the day when typically the traffic levels are more or less constant.

An average of the attenuation coefficient for the entire measurement time was calculated. The Bond correction, described in section 2.3, was applied to the attenuation coefficient. The values used were $CF_{PSAP} = 2$ and $MAC^{637} = 10$ m^2/g. Since the scattering coefficient is not known, two extremes were applied: $\sigma_{sp,1} = 0$ Mm^{-1} which corresponds to no scattering, and $\sigma_{sp,1} = 33$ Mm^{-1} which is a high scattering value measured in Spain (Mogo et al. 2017) which has a lot of airborne dust. The scattering coefficient from Spain is measured at 550 nm (Mogo et al. 2017), which is 25 nm longer than what the PSAP operated at, but the probable scattering source is dust particles which have a very low dependence on the wavelength (Pandolfi et al. 2017) so it should still be relevant. The resulting carbon mass concentrations are presented in table 2.

	high σ_{sp}	low σ_{sp}
Street level (2017/02/16)	0.610 µg/m^3	0.633 µg/m^3
Street level (2017/02/28)	0.100 µg/m^3	0.122 µg/m^3
Urban background (2016/11/27)	-0.064 µg/m^3	-0.042 µg/m^3
Urban background (2016/11/29)	-0.017 µg/m^3	0.006 µg/m^3
Urban background (2016/12/07)	-0.028 µg/m^3	-0.006 µg/m^3

Table 2: The calculated carbon mass concentrations for the two different measurement sites and for two different scattering values.

As can be seen, the value of the scattering coefficient results in a relatively small difference of the carbon mass concentration. The fluctuations of the measured attenuation coefficient is probably a more significant error source than the scattering coefficient.

The cause for the negative values for the urban background site is unknown, but is probably due to the calibration. Though, the levels of both black carbon and scattering particles were also probably low the days those measurements

were taken. The reason for the distinctly different measurement values at street level could not be concluded based on the short time period of measurement.

Measurements from different cities can be used to compare to the street level black carbon concentration. In Hyderabad in India, a city with a population of 5.7 million, an average mass concentration of 12 µg/m^3 has been measured within the urban center, and Anantapur also in India, with 0.5 million inhabitants, has an average of 0.85 µg/m^3 measured at the southern edge of the city (Badarinath et al. 2008). In downtown Helsinki in Finland, with 630,000 inhabitants, an average black carbon concentration of 1.38 µg/m^3 has been measured (Pakkanena et al. 2000). Kermanshah is a city of 850,000 inhabitants. The measured value of 0.6 µg/m^3 and 0.1 µg/m^3 at street level is a little low compared to this, but in the same size range. One reason for the relatively low values ate that the measurements in Kermanshah are taken in the middle of the day, away from rush hours, when the traffic intensity is generally lower. Though, since the measurements in Kermanshah only are taken over a few hours, while the concentrations in the other cities are over a far longer time, direct comparisons are difficult to make.

OC/EC filters will soon be available to determine the specific MAC-value in Kermanshah, Iran. This will increase the accuracy of the black carbon mass concentration from the PSAP. The SMPS in Iran is almost completed, the only component missing is the charger. Though, this is actively worked upon, and hopefully the SMPS system will be operational shortly. A cascade impactor is also being set up for usage, providing an ability to measure the mass size distribution.

The Aerosol Association in the Middle East and North Africa (AAMENA), is a network for aerosol research in the Middle East and North Africa. Its co-chairs are Professor Najat Saliba and Professor Tareq Hussein, and it was created 2014. Its objectives are: to raise the awareness of air pollution in the region, promote aerosol research and collaboration in the region, being a scientific body for policy makers, and being a link between researchers and international environmental agencies as WHO, WMO, and more (Terradellas 2017). There are plans to join this network. This will in time increase the coverage of measurements of aerosol particles, for the sake of both the climate and health effects.

5 Conclusions

To reiterate, the Lund SMPS is restored to working order, but still has some improvements that can be implemented.

Putting together an SMPS system at Razi University to be able to measure the number size distribution there is under way, and will probably be finalized shortly. Routines to calibrate the SMPS has been set up to facilitate the process at Razi University.

The black carbon concentration of around 0.6 µg/m^3 at street level is low, but not unreasonable. This might be due to the short duration of the measurements, them taking place outside of rush hour. To get a more thorough understanding of the black carbon levels and fluctuations, further and more long lasting measurements should be conducted. Preferably two PSAP should be available to measure the street level concentration and the background concentrations simultaneously. Hopefully, soon a cascade impactor and an SMPS will be able to be used for further measurements in Kermanshah, Iran.

References

Arnott, W. P. et al. (2006). "Photoacoustic insight for aerosol light absorption aloft from meteorological aircraft and comparison with particle soot absorption photometer measurements: DOE Southern Great Plains climate research facility and the coastal stratocumulus imposed perturbation experiments". In: *Journal of Geophysical Research: Atmospheres* 111 (D5). DOI: 10.1029/2005JD005964.

Badarinath, K. V. S. et al. (2008). "Black carbon aerosol mass concentration variation in urban and rural environments of India – a case study". In: *Atmospheric science letters* 10, pp. 29–33. DOI: 10.1002/asl.206.

Blanco, A. et al. (2003). "Characterization of African dust over southern Italy". In: *Atmospheric Chemistry and Physics* 3, pp. 2147–2159. DOI: 10.5194/acp-3-2147-2003.

Dall'Osto, M. et al. (2008). "A Study of the Size Distributions and the Chemical Characterization of Airborne Particles in the Vicinity of a Large Integrated Steelworks". In: *Aerosol Science and Technology* 42.12. DOI: http://dx.doi.org/10.1080/02786820802339587.

Dedering, Uwe (2008). *Iran relief location map*. URL: https://commons.wikimedia.org/wiki/File:Iran_relief_location_map.jpg#filelinks (visited on 05/22/2017).

Flagan, R. C. (2011). "Aerosol Measurement: Principles, Techniques, and Applications". In: John Wiley and Sons, Inc. Chap. 15 Electrical Mobility methods for submicrometer particle characterization, pp. 339–364.

Gharibi, A. (2006). "Studies of aerosol particle formation from various sources using ion and electron beam analytical techniques". Department of Physics.

Hinds, W. C. (1999a). "Aerosol Technology". In: John Wiley and Sons, Inc. Chap. 1 Introduction, pp. 3–13.

— (1999b). "Aerosol Technology". In: John Wiley and Sons, Inc. Chap. 11 Respiratory Deposition, pp. 233–247.

— (1999c). "Aerosol Technology". In: John Wiley and Sons, Inc. Chap. 2 Properties of gases, pp. 15–41.

Huang, J. et al. (2014). "Climate effects of dust aerosols over East Asian arid and semiarid regions". In: *Journal of Geophysical Research* 119.19, pp. 11, 398–11, 416. DOI: 10.1002/2014JD021796.

Hussein, T. et al. (2011). "Local Air Pollution versus Short–range Transported Dust Episodes: A Comparative Study for Submicron Particle Number Concentration". In: *Aerosol and Air Quality Research* 11, pp. 109–119. DOI: 10.4209/aaqr.2010.08.0066.

Jokinen, V. and J. M. Mäkelä (1996). "Closed-loop Arrangement with Critical Orfice for DMA Sheath/Excess Flow System". In: *Journal of Aerosol Science* 28.4, pp. 643–648.

Kristensson, A. (2003). "Characterization of sources of aerosol particles affecting Swedish air quality". Department of Physics.

Lihavainen, H. et al. (2016). "Aerosols physical properties at Hada Al Sham, western Saudi Arabia". In: *Atmospheric Environment* 135, pp. 109–117. DOI: http://doi.org/10.1016/j.atmosenv.2016.04.001.

Mogo, S. et al. (2017). "Comparison between the optical properties of aerosols in the fine and coarse fractions over Valladolid, Spain". In: *Environmental Science: Processes & Impacts* 19, pp. 123–133. DOI: 10.1039/C6EM00629A.

NASA (2017). *Aerosol transport and assimilation*. URL: https://gmao.gsfc.nasa.gov/research/aerosol/ (visited on 04/25/2017).

Pakkanena, T. A. et al. (2000). "Atmospheric black carbon in Helsinki". In: *Atmospheric Environment* 34 (9), pp. 1497–1506. DOI: https://doi.org/10.1016/S1352-2310(99)00344-1.

Pandolfi, M. et al. (2017). "A European aerosol phenomenology-6: Scattering characteristics of atmospheric aerosol particles from 28 ACTRIS sites".

Roumie, M. et al. (2016). "Evaluation and mapping of PM2.5 atmospheric aerosols in Arasia region using PIXE and gravimetric measurements". In: *Nuclear Instruments and Methods in Physics Research Section B: Beam Interactions with Materials and Atoms* 371, pp. 381–386. DOI: http://doi.org/10.1016/j.nimb.2015.12.034.

SMHI (2011). *Aerosol modelling*. URL: http://www.smhi.se/en/research/research-departments/air-quality/aerosol-modelling-1.5397 (visited on 02/14/2017).

Terradellas, E. (2017). *Aerosol Association in the Middle East - Northern Africa Region*. URL: https://sds-was.aemet.es/projects-research/aerosol-association-in-the-middle-east-northern-africa-region (visited on 05/18/2017).

Terradellas, E., S. Nickovic, and X.-Y. Zhang (2015). "Airborne Dust: A Hazard to Human Health, Environment and Society". In: *Bulletin* 64.2. URL: https://public.wmo.int/en/resources/bulletin/airborne-dust-hazard-human-health-environment-and-society (visited on 04/10/2017).

Tiitta, P. T. (2009). "The physical and chemical properties of traffic related and biogenic aerosols". Department of Physics.

TSI (1999). *Model 3010 Condensation Particle Counter*. URL: http://www.tsi.com/uploadedFiles/_Site_Root/Products/Literature/Spec_Sheets/3010.pdf (visited on 02/24/2017).

Wang, S. C. and R. C. Flagan (1990). "Scanning Electrical Mobility Spectrometer". In: *Aerosol Science and Technology* 13.2, pp. 230–240. DOI: 10.1080/02786829008959441.

WHO (2017). *Ambient (outdoor) air quality and health*. URL: http://www.who.int/mediacentre/factsheets/fs313/en/ (visited on 06/12/2017).

Xie, R. K. et al. (2005). "Chemical characterization of individual particles (PM10) from ambient air in Guiyang City, China". In: *Science of The Total Environment* 343, pp. 261–272. DOI: 10.1016/j.scitotenv.2004.10.012.

Zanatta, M. et al. (2016). "A European aerosol phenomenology-5: Climatology of black carbon optical properties at 9 regional background sites across Europe". In: *Atmospheric Environment* 145, pp. 346–364. DOI: http://dx.doi.org/10.1016/j.atmosenv.2016.09.035.

Appendices

A Instructions for testing the sheath flow pump

The aim of testing the pump is to determine if it performs to the expected levels. The set up for testing the pump is depicted in figure A1

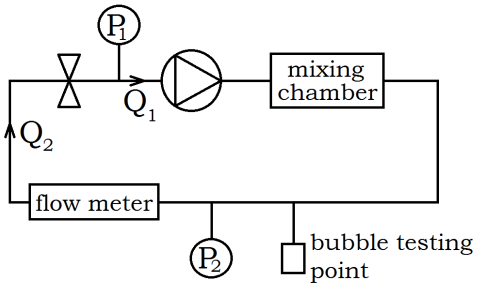

Figure A1: Overview of the pump testing setup. The P in the figure denotes the local pressure and Q the flow.

The mixing chamber eliminates the pulsating flow from the pump, and the needle is used to regulate the flow. The bubble testing point is used to test how stable the pump is by putting a bubble of liquid over the protruding tube and checking that it does not move significantly.

To see if the pump preforms to the values set by the producer, the values from the performed test can be compared to a graph from the producer. An example of such a graph can be seen in figure A2.

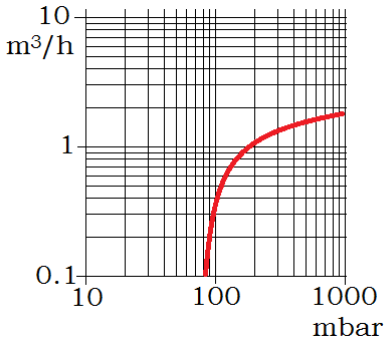

Figure A2: Curve for a pump with flow on the y-axis and pumped pressure on the x-axis.

Use the needle valve to regulate the pressure and flow. Compare the resulting values with the ones from the producer. The pump will usually be a bit lower

than the producers' specifications, but if it is much lower it needs to be serviced.

Often the producers use the flow at the pressure P_1, Q_1, and not at the atmospheric pressure, P_2. We will have to use the ideal gas law to convert the producers' specified flow at P_1 to our measured flow, P_2. This is done by:

$$P_1 \cdot \frac{\Delta V_1}{\Delta t} = P_2 \cdot \frac{\Delta V_2}{\Delta t} \tag{A2}$$

where P_1 and P_2 are the pressures as specified in figure A1 and V_1 and V_2 are the volumes on the two sides of the needle valve and the pump. Rewritten this becomes:

$$Q_2 = \frac{P_1 \cdot Q_1}{P_2} \tag{A2}$$

B Instructions for calibration of the voltage output

The voltage output needs to be calibrated to make sure that the voltage that the SMPS-program specifies is the voltage actually applied in the DMA.

The computer should be connected to the voltage supplier, but the voltage supplier should not be connected to the DMA. Open the "Measurement & Automation explorer" on the computer. There you open "Data neighborhood" in the leftmost menu, and thereafter select the "Global virtual channels" option. Then choose the global channel that you want to calibrate. In figure B1 a screen cap of the Measurement & Automation explorer with the relevant channel open can be seen.

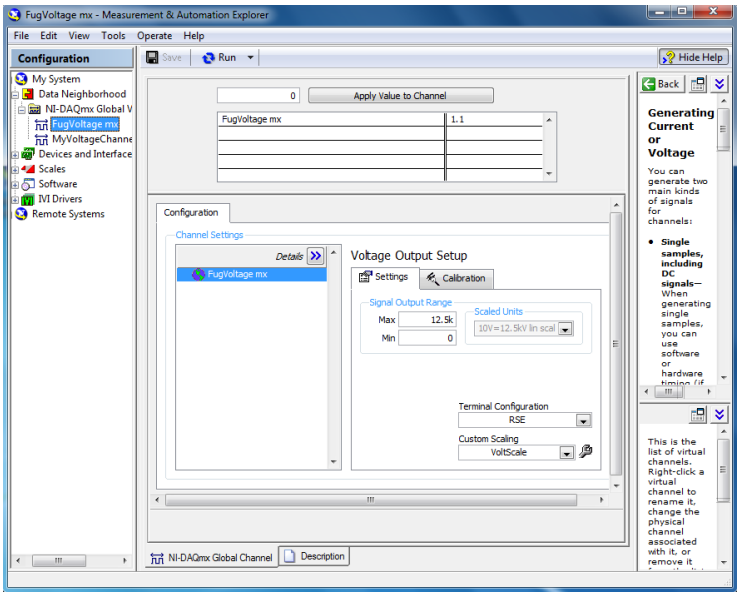

Figure B1: Screen shot of the Measurement & Automation explorer with the channel chosen.

Enter a voltage value into the top left box and press "apply value to channel" and "run". Measure the output voltage from the voltage supplier with a volt meter. The output should be within 2 % of the set voltage. If it is not, you can create and edit a custom scaling. This can be done in the down right corner of the window in figure B1. This will open the window depicted in figure B2. Here you can set the slope and an offset for the scaling of the output voltage until it is within the desired range.

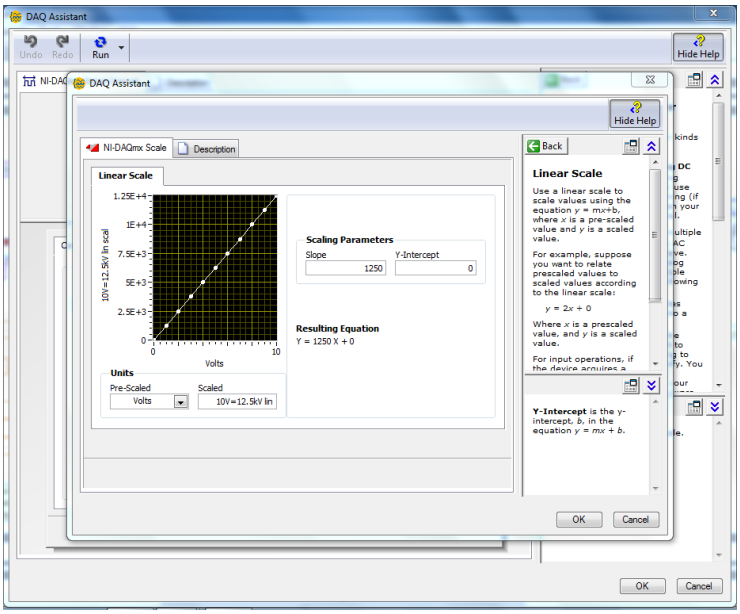

Figure B2: Screen shot of the Measurement & Automation explorer in the custom scaling window

C Instructions for size calibration of the SMPS

To perform the size calibration of the SMPS, aerosol particles of a known size need to be generated. This is usually done with Polystyrene Latex (PSL) spheres, which can be bought in a multitude of different sizes. The setup for how to aerosolize these PSL particles can be seen in figure C1.

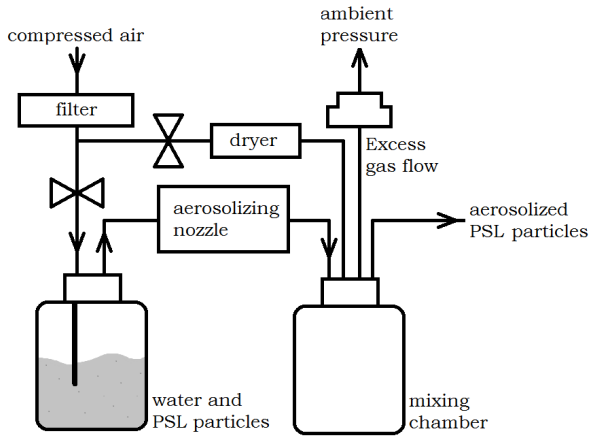

Figure C1: Setup for aerosolizing PSL particles.

Air at a high pressure is passed through a filter to remove all preexisting particles from the air flow. The needle valve is used to regulate the pressure entering the system. The high pressure air enters a liquid through a nozzle. The liquid consists of purified water and PSL spheres of a known size. Here water droplets containing PSL particles are produced. They travel with the air flow into an aerosolizing nozzle that generates aerosols with only one PSL sphere per aerosol. Thereafter the air flow enters the mixing chamber where clean and dried compressed air can be let in through a needle valve to dilute the aerosol gas to desired concentrations. At the same time the aerosol particles are dried. From there the aerosol can enter the SMPS and the excess gas will leave the mixing chamber through a filter. This prevents high pressure in the SMPS.

With this setup running, do a complete scan with the SMPS. The peak that can be seen in the scan should be centered around the size of the used PSL spheres. If the sizes do not agree, check that all the flows and the DMA dimensions are correct in the SMPS program. If everything is in order and the difference still remains, the difference should be noted whenever the SMPS is used for measurements.

D Instructions for number calibration of the SMPS

The most simple way to calibrate the total number concentration for an SMPS system is to use compare the concentration to the CPC concentration measured with the same CPC as in the SMPS.

Measure a polydisperse aerosol with the SMPS. Compare the concentration with one measured with the CPC which is directly connected to the aerosol. The number concentration from the SMPS and the CPC will rarely be exactly the same but should be within 10-20 % of each other.

This calibration can be performed either by measuring a generated polydisperse aerosol, or the ambient air. Though, if performed on the ambient air it needs to be a day with few to no particles with a diameter below 20 nm. These particles are difficult to treat in the SMPS program, in the inversion routine, and can give a difference in the number concentration even though there is not anything wrong with the SMPS.